Title: Risk of pesticide pollution at the global scale

Authors: Fiona H.M. Tang[1,*], Manfred Lenzen[2], Alexander McBratney[3], & Federico Maggi[1,*]

Affiliations: [1]Environmental Engineering, School of Civil Engineering, The University of Sydney, 2006, Sydney, NSW, Australia. [2]ISA, School of Physics A28, The University of Sydney, NSW 2006, Australia. [3]Sydney Institute of Agriculture, The University of Sydney, 2006, Sydney, NSW, Australia.
[*]Corresponding author.

Pesticides are widely used to protect food production and meet global food demand but are also ubiquitous environmental pollutants, causing adverse effects on water quality, biodiversity, and human health. Here we use a global database of pesticide applications and a spatially-explicit environmental model to estimate the world geography of environmental pollution risk caused by 92 active ingredients in 168 countries. We considered a region be at risk of pollution if pesticide residues in the environment exceeded the no-effect concentrations and be at high risk if exceeded by three orders of magnitude. We find that 64% of global agricultural land (~ 24.5 million km^2) is at risk of pesticide pollution by more than one active ingredient, and 31% is at high risk. Among the high-risk areas, about 34% are in high biodiversity regions, 5% in water-scarce areas, and 19% in low- and lower-middle-income nations. We identify watersheds in South Africa, China, India, Australia, and Argentina as high concern regions because they have high pesticide pollution risk, bear high biodiversity, and suffer from water scarcity. Our study expands earlier pesticide risk assessments as it detailly accounts for multiple active ingredients and integrates risks in different environmental compartments at a global extent.

Agrochemicals such as synthetic fertilizers and pesticides have together made a remarkable contribution to food security in the last 50 years[1]. Notwithstanding the increased food availability[2], the unpreventable ubiquity of agrochemicals throughout the environment has resulted in pollution and has negatively impacted the ecosystem and human health[3-5]. However, in contrast to the global awareness of the environmental footprint related to fertilizers[6,7], the global repercussions of pesticide dispersion in the environment remain largely unknown due to the lack of a comprehensive geographic quantification of active ingredient (AI) use and residues. Studies addressing pesticide threats mostly remain site-specific, and only a minority have targeted regional and global extents[8-11] to assess the risks associated with a specific pesticide class (e.g., insecticides or organochlorine pesticides) or within a certain environmental compartment (e.g., surface water[8,10] and atmosphere[12,13]). Given the expected population growth, the use of agricultural pesticides will likely continue to increase in the future[5]; yet, in the age of globalization, a global outlook of environmental pollution by pesticides and its relation to ecosystem vulnerability is still missing.

To contribute to filling in this gap, we propose the global mapping of the environmental risks posed by the 92 most used AIs (comprising 59 herbicides, 21 insecticides, and 19 fungicides) at 5 arc-minutes resolution (about 10 km ×10 km at the equator), which we next juxtaposed to water-scarcity[14], biodiversity[15-18], and national income[2]. Our assessment targets the ecological risks in four environmental compartments, namely, soil, surface water, groundwater, and atmosphere, noting that we did not include pesticide impacts on human health and not all living organisms in an environmental compartment are considered. Based upon these analyses, we ultimately identified susceptible regions that may require tailored strategies for sustainable use of pesticides in agriculture.

Pesticide risk in global agricultural land

To quantify pesticide risk in each geographic grid cell, we calculated the non-cumulative Predicted Environmental Concentration (PEC) of each targeted AI in the four environmental compartments mentioned above using a spatially explicit model[19] fed with geo-referenced environmental data sets and AI physicochemical properties as inputs (Methods, Supplementary Information Table S1 and Table S2). We sourced the geographic- and crop- specific AI application rates from our recently developed PEST-CHEMGRIDSv1[20] global database gridded at 5 arc-minutes resolution (Methods). In each grid cell, the agricultural land consists of multiple crop types[21] that receive applications of multiple AIs[20]. Hence, we adopted the hierarchical approach of the PURE decision-support system[22], which sums the risk quotient of all AIs within an environmental compartment. The risk quotient was determined as the ratio between PEC and the Predicted No-Effect Concentration (PNEC) derived from each AI's ecotoxicities (Methods, Supplementary Information Table S2). The "risk point" of each environmental compartment was then evaluated as the log-transformed sum of all risk quotients. Finally, the overall "risk score" in a grid cell (RS) was calculated as the maximum risk point across the four environmental compartments. Based on the species sensitivity distribution curve (Methods, Supplementary Information Fig. S1), we classified RS into negligible ($RS \leq 0$), low ($0 < RS \leq 1$), medium ($1 < RS \leq 3$), and high ($RS > 3$) risk. This procedure allows us to draw a global picture of environmental susceptibility to pesticide pollution.

Specifically, we find that 74.8% of the global agricultural land (approximately 28.8 million km^2) is at some risk of pesticide pollution (i.e., $RS > 0$, Fig. 1); remarkably, 31.4% (approximately 12.1 million km^2) falls within the high-risk class (i.e., $RS > 3$). Regional analysis shows that 61.7% (2.3 million km^2) of the European agricultural land is at high risk of pesticide pollution. The three European countries with the largest land area of high risk are located in Eastern and Southern Europe, namely, Russia (0.91 million km^2, Supplementary Information Table S4), Ukraine (0.35 million km^2, Supplementary Information Table S4), and Spain (0.19 million km^2, Supplementary Information Table S4), which are among the largest crop producers in Europe[21]. Among all regions, Asia has the largest land area at high risk (4.9 million km^2), with 2.9 million km^2 being in China and 0.35 million km^2 in Kazakhstan (Supplementary Information Table S4). The agricultural land in Oceania shows the lowest pesticide pollution risk.

Our pesticide risk score map in Fig. 1 complements and expands earlier assessments such as the insecticide runoff potential analysis in Ippolito et al. (2015)[8], which identifies similar high-risk regions in Asia, America, and South Europe. However, the accounting of a wider range of pesticide AIs and environmental compartments in this work reveals additional geographic regions undergoing high pollution risk, for example, areas across Eastern Europe and parts of Africa where the earlier assessment reports medium to very low runoff potential[8].

Pollution by pesticide mixtures is an emerging global issue because mixtures can elicit synergistic toxicity in non-target organisms under both acute and chronic exposures[23,24]. The risk map in Fig. 1 considers their additive effects, but excludes synergistic effects; hence, to better illustrate the global extent of pollution by pesticide mixtures, we counted the AIs that pose risks to the environment in each grid cell. An AI is considered to pose a risk when its PEC in any environmental compartment exceeds PNEC. Globally, 63.7% of the agricultural land is at risk of pollution by more than one AI and 20.9% by more than 10 AIs (Fig. 2). We find that 93.7%, 73.4%, and 69.4% of the agricultural land in Europe, North America, and South America, respectively, are contaminated by more than one AI. China is at risk of pollution by the greatest number of AIs, with 8.4% of the agricultural land (0.34 million km^2, Supplementary Information Table S5) being contaminated by more than 20 AIs.

Pesticide risk in vulnerable regions

Pesticides can be transported to surface waters and groundwater through runoffs and infiltration, causing pollution to water bodies, thus, reducing the usability of water resources. By mapping the pesticide risk and AI count over the water risk database in AQUEDUCT-v2.1[14], we find that, globally, 0.62 million km^2 of agricultural land in regions suffering from highly variable and scarce water supply are facing high pollution risk by pesticide mixtures, among which 20.1% are located in low- and lower-middle-income countries (Extended Data Fig. 1a). Nation-wise, China has the most extensive land area subject to water scarcity and high pesticide pollution risk (0.27 million km^2, i.e., about 3% of China's total land surface, Extended Data Fig. 1a and Supplementary Information Fig. S2a), with surface water appearing to be the most susceptible environmental compartment (Extended Data Fig. 2). In contrast, groundwater is relatively protected from pesticide pollution (Extended Data Fig. 2) due to low aquifer net recharge.

To assess if pesticide use constitutes a threat to biodiversity, we analysed the pesticide risk and AI count maps against geographically-gridded species richness for tetrapods, which include mammals[16], birds[15], amphibians[17], and reptiles[18]. We find that 34.1% of the global high pesticide pollution risk areas (approximately 4.18 million km^2) are located in regions bearing high biodiversity (i.e., ≥ 323 tetrapod species, the 75th percentile of global value), with 1.25 million km^2 being in low- and lower-middle-income countries (Extended Data Fig. 1b). As the decline in amphibians has earlier been tightly linked to pesticide contamination[25], we expanded our analysis to highlight the exposure of vulnerable amphibian species to pesticide pollution risk. We find that 0.37 million km^2 of areas at risk of pesticide mixture pollution (i.e., RS > 0 and AI count > 1) intersect the habitat of at least one of either endangered or critically endangered amphibian species (Extended Data Fig. 1c), with major hotspots located in China, Australia, Guatemala, and Chile. Along with many studies underlining the toxicity of pesticides to wildlife[26], the biodiversity loss earlier associated to the export of agricultural products that led to deforestation and habitat loss[27] finds in our analysis an additional element of attention; that is, pesticide dispersion in intensive agriculture is an additional stressor that can exacerbate the loss of biodiversity.

Regions of concern

To represent our work in synthesis, we integrated the indicators for pesticide pollution risk, water scarcity, and biodiversity into a map that locates regions of concern where tailored strategies for sustainable use of pesticides may be needed (Fig. 3). In this map, concern level 1 identifies regions of high pollution risk, high water scarcity, and high biodiversity. We identify the top five watersheds perceiving a level 1 concern as Orange in South Africa, Huang He in China, Indus in India, Murray in Australia, and Parana in Argentina. Surprisingly, four out of the five countries with level 1 concern are within the high- and upper-middle-income economies. Although the level 1 concern regions cover less than 30,000 km^2 of the land surface, we find 5.20 million km^2 perceives a level 2 concern and spreads mainly across Asia and South America, with 1.72 million km^2 located in low- and lower-middle-income countries.

Results in our study report a widespread global pesticide pollution risk with vast risk areas located in vulnerable regions that bear high biodiversity and suffer from low availability of freshwater supply. Our results expand and complement earlier regional-scale studies that report the detection of pesticide residues in freshwater bodies in South Africa[28] and the Yellow River (Huang He) in China[29]. Besides impacting ecosystem health, the leaching of pesticides to water bodies used as sources of drinking water can pose risks to human health. Our analysis supports the need for a more detailed global assessment of pesticide contamination levels in major rivers, estuaries, and lakes and to account for pollutant levels when assessing water scarcity and quality[30].

In a warmer climate with a growing population, the use of pesticides is foreseen to increase for combating the possible rise in pest invasions and for feeding the planet[31]; thus, the threats estimated in our study may escalate further. While protecting food production is essential for human development, reducing pesticide pollution is equivalently crucial to protect biodiversity that maintains soil health and functions contributing towards food security[32]. The increasing public awareness of the adverse impact of pesticides in recent years has pushed for the establishment of pesticide policies to reduce pesticide use. Within the context of policymaking, the spatial-explicit risk scores estimated in this study can provide an indicator to quantify pesticide risk in different agricultural settings (i.e., not merely the quantity of AIs used), which is currently missing in most of the pesticide policy frameworks[33]. The risk scores defined here align with the Pesticide Load indicators used in Denmark[34], though we did not account for pesticide impacts on human health. As our estimates extend globally across 168 nations, the proposed risk scores, AI counts, and the assessment of regions of concern can be incorporated into the Environmental Performance Index framework, which provides global metrics to rank countries' performance on sustainability issues[35].

Although this study has a sole focus on environmental health, the effect of pesticides on human health is also an important aspect that requires a comprehensive assessment. This assessment at a global scale is, however, highly intricate as it involves the quantification of human exposure to pesticides resulting from agricultural production and possible intake via diverse pathways including air, water, and food, where the latter intake pathway involves food distribution and international food trading. Hence, pesticide use can affect not only the health of local communities but also the consumers in other importing countries. We therefore urge to establish a global strategy to transition towards sustainable agriculture and sustainable living with low pesticide inputs and reduced food loss and food waste to achieve responsible production and consumption in an acceptable, profitable system.

References

1 Oerke, E. C. Crop losses to pests. *J. Agric. Sci.* **144**, 31-43 (2006).

2 FAOSTAT. Database Collection of the Food and Agriculture Organization of the United Nations. http://www.fao.org/faostat/en/#data (2019).

3 Beketov, M. A., Kefford, B. J., Schäfer, R. B. & Liess, M. Pesticides reduce regional biodiversity of stream invertebrates. *Proc. Natl. Acad. Sci. U.S.A.* **110**, 11039-11043 (2013).

4 Nicolopoulou-Stamati, P., Maipas, S., Kotampasi, C., Stamatis, P. & Hens, L. Chemical pesticides and human health: the urgent need for a new concept in agriculture. *Front. Public Health* **4**, 148 (2016).

5 Tilman, D. et al. Forecasting agriculturally driven global environmental change. *Science* **292**, 281-284 (2001).

6 Bouwman, A., Boumans, L. & Batjes, N. Modeling global annual N_2O and NO emissions from fertilized fields. *Global Biogeochem. Cycles* **16**, 28-21-28-29 (2002).

7 Cordell, D., Drangert, J. O. & White, S. The story of phosphorus: global food security and food for thought. *Glob. Environ. Change* **19**, 292-305 (2009).

8 Ippolito, A. et al. Modeling global distribution of agricultural insecticides in surface waters. *Environ. Pollut.* **198**, 54-60 (2015).

9 Silva, V. et al. Pesticide residues in European agricultural soils–A hidden reality unfolded. *Sci. Total Environ.* **653**, 1532-1545 (2019).

10 Stehle, S. & Schulz, R. Agricultural insecticides threaten surface waters at the global scale. *Proc. Natl. Acad. Sci. U.S.A.* **112**, 5750-5755 (2015).

11 Maggi, F., la Cecilia, D., Tang, F. H. M. & McBratney, A. The global environmental hazard of glyphosate use. *Sci. Total Environ.***717**, 137167 (2020).

12 Li, Y. F., Scholtz, M. T. & Van Heyst, B. J. Global gridded emission inventories of β-hexachlorocyclohexane. *Environ. Sci. Technol.* **37**, 3493-3498 (2003).

13 Shunthirasingham, C. et al. Spatial and temporal pattern of pesticides in the global atmosphere. *J. Environ. Monit.* **12**, 1650-1657 (2010).

14 Gassert, F., Luck, M., Landis, M., Reig, P. & Shiao, T. *Aqueduct global maps 2.1: Constructing decision-relevant global water risk indicators* (World Resources Institute, Washington, DC, 2014).

15 BirdLife International and Handbook of the Birds of the World. Bird species distribution maps of the world. Version 2019.1, http://datazone.birdlife.org/species/requestdis (2019).

16 International Union for Conservation of Nature (IUCN) & Center for International Earth Science Information Network (CIESIN) Columbia University. Gridded Species Distribution: Global Mammal Richness Grids, 2015 Release, NASA Socioeconomic Data and Applications Center (SEDAC) http://dx.doi.org/10.7927/H4N014G5 (2015).

17 International Union for Conservation of Nature (IUCN) & Center for International Earth Science Information Network (CIESIN) Columbia University. Gridded Species Distribution: Global Amphibian Richness Grids, 2015 Release, NASA Socioeconomic Data and Applications Center (SEDAC) http://dx.doi.org/10.7927/H4RR1W66 (2015).

18 Roll, U. et al. The global distribution of tetrapods reveals a need for targeted reptile conservation. *Nat. Ecol. Evol.* **1**, 1677 (2017).
19 Trevisan, M., Di Guardo, A. & Balderacchi, M. An environmental indicator to drive sustainable pest management practices. *Environ. Model. Softw.* **24**, 994-1002 (2009).
20 Maggi, F., Tang, F. H. M., la Cecilia, D. & McBratney, A. PEST-CHEMGRIDS, global gridded maps of the top 20 crop-specific pesticide application rates from 2015 to 2025. *Sci. Data* **6**, 1-20 (2019).
21 Monfreda, C., Ramankutty, N. & Foley, J. A. Farming the planet: 2. Geographic distribution of crop areas, yields, physiological types, and net primary production in the year 2000. *Global Biogeochem. Cycles* **22**, 1 (2008).
22 Zhan, Y. & Zhang, M. PURE: A web-based decision support system to evaluate pesticide environmental risk for sustainable pest management practices in California. *Ecotoxicol. Environ. Saf.* **82**, 104-113 (2012).
23 Maloney, E., Morrissey, C., Headley, J., Peru, K. & Liber, K. Can chronic exposure to imidacloprid, clothianidin, and thiamethoxam mixtures exert greater than additive toxicity in Chironomus dilutus? *Ecotoxicol. Environ. Saf.* **156**, 354-365 (2018).
24 Pape-Lindstrom, P. A. & Lydy, M. J. Synergistic toxicity of atrazine and organophosphate insecticides contravenes the response addition mixture model. *Environ. Toxicol. Chem.* **16**, 2415-2420 (1997).
25 Davidson, C., Shaffer, H. B. & Jennings, M. R. Spatial tests of the pesticide drift, habitat destruction, UV-B, and climate-change hypotheses for California amphibian declines. *Conserv. Biol.* **16**, 1588-1601 (2002).
26 Köhler, H. R. & Triebskorn, R. Wildlife ecotoxicology of pesticides: can we track effects to the population level and beyond? *Science* **341**, 759-765 (2013).
27 Lenzen, M. et al. International trade drives biodiversity threats in developing nations. *Nature* **486**, 109 (2012).
28 Ansara-Ross, T. M., Wepener, V., Van den Brink, P. J. & Ross, M. J. Pesticides in South African fresh waters. *Afr. J. Aquat. Sci.* **37**, 1-16 (2012).
29 Li, J., Li, F. & Liu, Q. Sources, concentrations and risk factors of organochlorine pesticides in soil, water and sediment in the Yellow River estuary. *Mar. Pollut. Bull.* **100**, 516-522 (2015).
30 van Vliet, M. T., Flörke, M. & Wada, Y. Quality matters for water scarcity. *Nat. Geosci.* **10**, 800-802 (2017).
31 Deutsch, C. A. et al. Increase in crop losses to insect pests in a warming climate. *Science* **361**, 916-919 (2018).
32 McBratney, A., Field, D. J. & Koch, A. The dimensions of soil security. *Geoderma* **213**, 203-213 (2014).
33 Möhring, N. et al. Pathways for advancing pesticide policies. *Nat. Food* **1**, 535-540 (2020).
34 Kudsk, P., Jørgensen, L. N. & Ørum, J. E. Pesticide Load—A new Danish pesticide risk indicator with multiple applications. *Land Use Policy* **70**, 384-393 (2018).
35 Wendling, Z. A. et al. *2020 Environmental Performance Index* (Yale Center for Environmental Law & Policy, New Haven, CT, 2020).

Corresponding authors
Correspondence to Fiona H.M. Tang (fiona.tang@sydney.edu.au) or Federico Maggi (federico.maggi@sydney.edu.au)

Acknowledgments
This work is supported by the University of Sydney through the SREI2020 EnviroSphere research program. F.M. is also supported by the SOAR Fellowship awarded by the University of Sydney. The authors thank Giovanni Porta for the discussion and advice on the uncertainty analysis. The authors acknowledge the Sydney Informatics Hub and the University of Sydney's high performance computing cluster Artemis for providing the high performance computing resources that have contributed to the results reported within this work. The authors acknowledge the use of the National Computational Infrastructure (NCI) which is supported by the Australian Government, and accessed through the Sydney Informatics Hub HPC Allocation Scheme supported by the Deputy Vice-Chancellor (Research), the University of Sydney and the ARC LIEF, 2019: Smith, Muller, Thornber et al., Sustaining and strengthening merit-based access to National Computational Infrastructure (LE190100021). We thank Rupert Hough and Matthias Liess for constructive comments on this manuscript.

Author contributions
F.H.M.T. and F.M have conceptualized the main research subject; F.H.M.T, M.L. and F.M. have contributed to data collection and analysis; F.H.M.T, M.L., A.M, and F.M. have contributed to the interpretation of the results and the writing of the manuscript. F.H.M.T, M.L., A.M, and F.M. have contributed to acquire funding for this work.

Competing interests
The authors declare no competing interests.

Figure captions
Fig. 1 Global map of pesticide risk scores (RS). RS ≤ 0 is classified as negligible risk, 0 < RS ≤ 1 as low risk, 1 < RS ≤ 3 as medium risk, and RS > 3 as high risk. The pie charts represent the fraction of agricultural land undergoing different risk scores in each region. Values in the brackets above the pie charts denote the total agricultural land in that region in million km^2. The map has a spatial resolution of 5 arc-minutes, which is approximately 10 km × 10 km at the equator.

Fig. 2 Global map of the number of active ingredients (AI) posing risks to the environment. The pie charts represent the fraction of agricultural land contaminated by different number of AIs in each region. Values in the brackets above the pie charts denote the total agricultural land in that region in million km^2. The map has a spatial resolution of 5 arc-minutes, which is approximately 10 km × 10 km at the equator.

Fig. 3 Global map of the regions of concern defined against pesticide pollution risk, water scarcity, and biodiversity. Regions of concern level 1 signify areas of high pesticide pollution risk, high water scarcity, and high biodiversity. They are indicated with red circles, followed by country, watershed name, and the impacted land area in km^2. The map has a spatial resolution of 5 arc-minutes, which is approximately 10 km × 10 km at the equator.

Extended Data Fig. 1 The top 30 countries susceptible to high pesticide pollution risk. a., The land area subject to low quantity and high variability of water supply and high risk of pollution by pesticide mixtures (i.e., RS > 3 and AI count > 1). **b.,** The land area bearing high biodiversity and subject to high risk of pollution by pesticide mixtures (i.e., RS > 3 and AI count > 1). **c.,** The land area inhabited by at least one endangered and critically endangered amphibian species and subject to pollution risk by pesticide mixtures (RS > 0 and AI count > 1).

Extended Data Fig. 2 The extent of pesticide pollution risk in groundwater, surface water, soil, and atmosphere expressed as percent agricultural land. For example, surface water within 74% of global agricultural land is at some risk of pesticide pollution. High water risk regions refer to places suffering from low quantity and high variability of water supply defined as in AQUEDUCT-v2.1 database.

Data availability

The georeferenced data that support the findings of this study are available in *figshare* with the identifier doi: 10.6084/m9.figshare.10302218[60]. Country-based data are distributed in tabulated format in the Supplementary Information file associated with this article.

Code availability

The code used to calculate pesticide risk scores is provided as a Matlab file available in *figshare* with the identifier doi: 10.6084/m9.figshare.10302218[60].

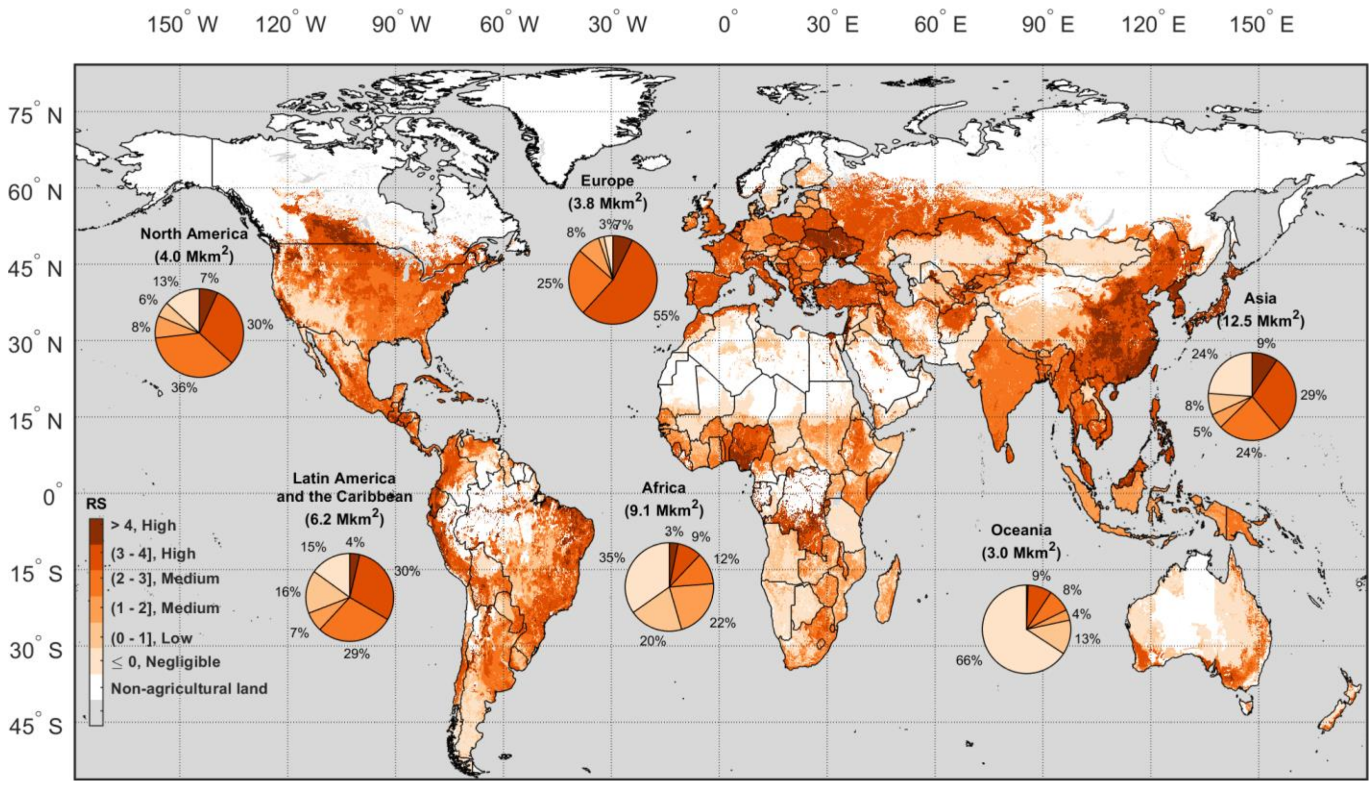

Fig. 1 Global map of pesticide risk scores (RS). RS ≤ 0 is classified as negligible risk, $0 < RS \leq 1$ as low risk, $1 < RS \leq 3$ as medium risk, and RS > 3 as high risk. The pie charts represent the fraction of agricultural land undergoing different risk scores in each region. Values in the brackets above the pie charts denote the total agricultural land in that region in million km^2. The map has a spatial resolution of 5 arc-minutes, which is approximately 10 km × 10 km at the equator.

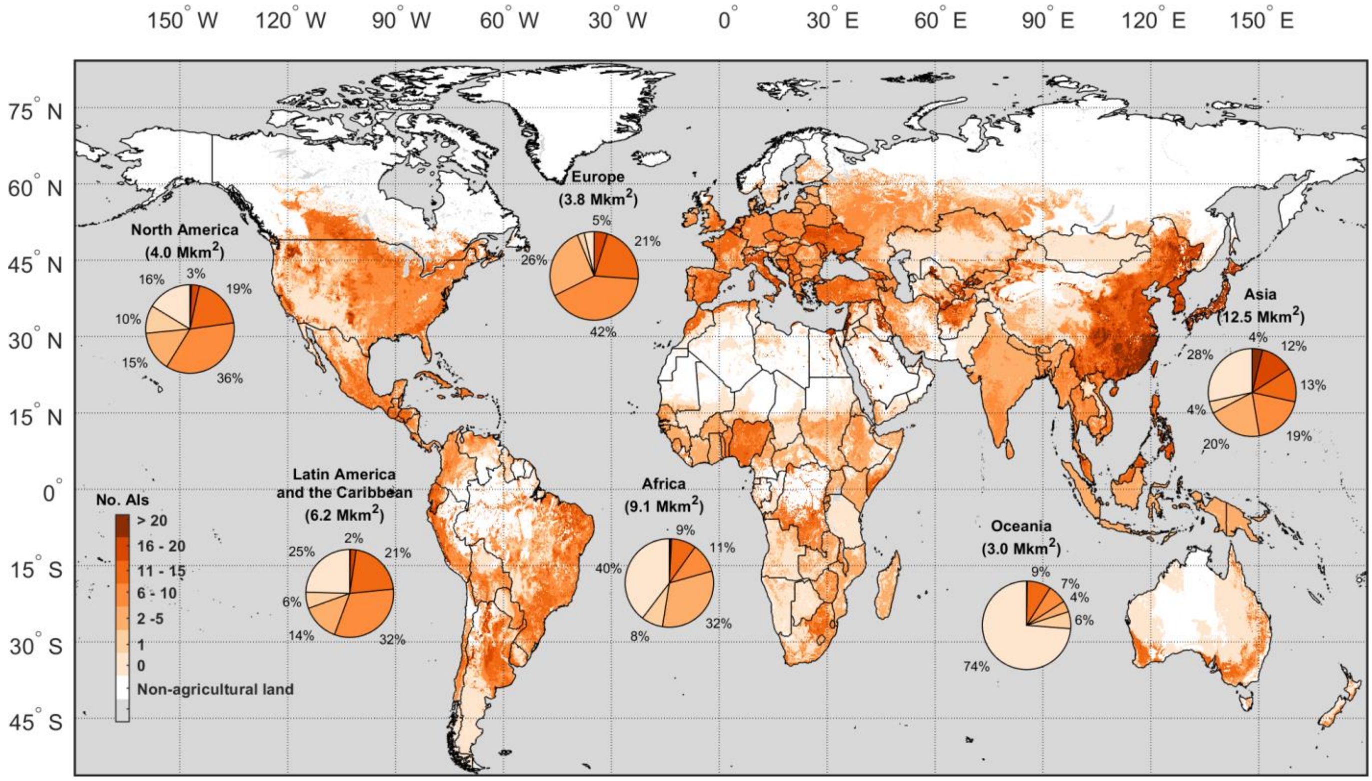

Fig. 2 Global map of the number of active ingredients (AI) posing risks to the environment. The pie charts represent the fraction of agricultural land contaminated by different number of AIs in each region. Values in the brackets above the pie charts denote the total agricultural land in that region in million km^2. The map has a spatial resolution of 5 arc-minutes, which is approximately 10 km × 10 km at the equator.

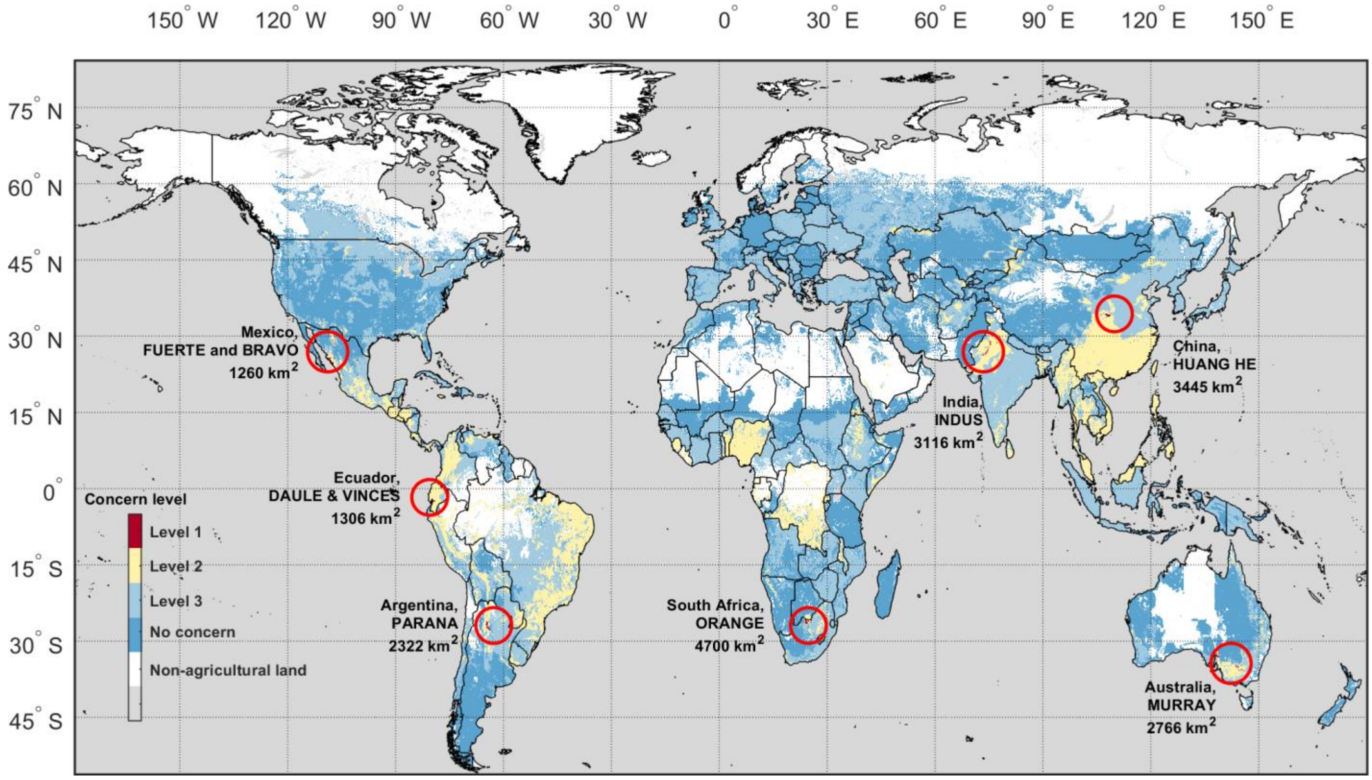

Fig. 3 Global map of the regions of concern defined against pesticide pollution risk, water scarcity, and biodiversity. Regions of concern level 1 signify areas of high pesticide pollution risk, high water scarcity, and high biodiversity. They are indicated with red circles, followed by country, watershed name, and the impacted land area in km^2. The map has a spatial resolution of 5 arc-minutes, which is approximately 10 km × 10 km at the equator.

Methods

All modelling and analyses were conducted using Mathworks MatlabR2017a.

Application rates of active ingredients. To determine pesticide pollution risks, we first predicted the pesticide concentrations in all environmental compartments, which implied knowledge of pesticide application rates. For this, we used our previous work (PEST-CHEMGRIDS[20]) to obtain the global georeferenced crop-specific active ingredients (AI) annual application rates in year 2015, which were estimated based on the data provided by the USGS Pesticide National Synthesis Project (USGS/ PNSP)[36] and constrained against the country-specific pesticide use data reported by FAOSTAT[2]. PEST-CHEMGRIDS provides the high and low estimates of the top 20 AIs used on 175 crops, classified into six dominant crops (alfalfa, corn, cotton, rice, soybean, and wheat) and four aggregated crop classes (vegetables and fruit, orchards and grapes, pasture and hay, and other crops), totalling 95 different AIs that represent about 84% of the pesticide mass used in 2015. Crops were aggregated based on the classification in the USGS Pesticide National Synthesis Project (USGS/ PNSP)[36] and were detailly described in Table 2 in ref[20]. In this study, we excluded three AIs (*Bacillus amyloliquefaciens*, calcium polysulfide, and petroleum oil) from PEST-CHEMGRIDS due to insufficient input data relative to their physicochemical properties and ecotoxicities. Hence, in the assessment of pesticide pollution risks, we accounted for the applications of 92 AIs in total (listed in Supplementary Information Table S2) on 10 crop classes at median annual rates.

Predicted environmental concentrations. Because the AI application history at a specific location was not known, we calculated the non-cumulative predicted environmental concentrations (PEC) of each AI in groundwater (GW), surface water (SW), soil (SL), and atmosphere (AT) using the spatially explicit approach of the EPRIP 2.1 (Environmental Potential Risk Indicator for Pesticide version 2.1)[19] with the assumption that all AIs were applied once a year at the annual application rates of 2015 obtained from PEST-CHEMGRIDS. The estimated PECs refer to those observed following an application and are not cumulated over time.

The non-cumulative PEC in groundwater ($\mathrm{PEC}_{i,j}^{\mathrm{GW}}$) of active ingredient *i* on crop *j* was calculated as a function of application rate $R_{i.j}$, soil properties (porosity, bulk density, field capacity, and organic carbon content), groundwater characteristics (water table depth, groundwater thickness, and net recharge rate), and AI physicochemical properties (degradation rate, volatility, and adsorption capacity). In surface water, $\mathrm{PEC}_{i,j}^{\mathrm{SW}}$ was calculated using the empirical approach in the SYNOPS[37] and DRIPS[38] models to account for $R_{i.j}$, topography (slope angle), rainfall depth, and the AI fraction available for transport via runoff determined by AI degradation rate and its adsorption to soil organic carbon. The PEC in soil, $\mathrm{PEC}_{i,j}^{\mathrm{SL}}$, at the top 2 cm depth was calculated as a function of $R_{i.j}$ and soil bulk density, and it was used to determine the AI atmospheric concentration $\mathrm{PEC}_{i,j}^{\mathrm{AT}}$. Using the approach in the VOLASOIL[39] model, we calculated $\mathrm{PEC}_{i,j}^{\mathrm{AT}}$ as a function of $\mathrm{PEC}_{i,j}^{\mathrm{SL}}$, soil properties (porosity, bulk density, field capacity, and organic carbon content), AI physicochemical properties (water solubility, volatility, and adsorption), and atmospheric temperature.

Predicted no-effect concentrations. We defined the predicted no-effect concentrations (PNEC) of the 92 selected AIs in each of the four environmental compartments using an assessment factor approach[40] with acute toxicity data sourced from the Pesticide Properties DataBase (PPDB)[41] (Supplementary Information Table S2). The PNECs in surface water and soil were determined using the LC50 of fishes and earthworms, respectively, with an assessment factor of 1,000, i.e., $\mathrm{PNEC}_i^{\mathrm{SW}} = \mathrm{LC50}_i^{\mathrm{fishes}}/1{,}000$ and $\mathrm{PNEC}_i^{\mathrm{SL}} = \mathrm{LC50}_i^{\mathrm{earthworms}}/1{,}000$. For the atmosphere, we defined PNEC as the inhalation LC50 of rats with an assessment factor of 1,000. Following the European Commission guidelines[42], we defined the PNEC for groundwater as 0.1 µg/L for all AIs with no assessment factor applied.

Pesticide pollution risks. For each environmental compartment *k*, we calculated the crop-specific risk quotient (RQ) of each AI as the ratio between PEC and PNEC (i.e., $\mathrm{RQ}_{i,j}^k = \mathrm{PEC}_{i,j}^k/\mathrm{PNEC}_i^k$). Because a specific AI can be used across multiple crop classes within a grid cell, we calculated the overall RQ of each AI by weight averaging the crop-specific RQs with the crop harvested areas *A* (i.e., $\mathrm{RQ}_i^k = \sum_j(\mathrm{RQ}_{i,j}^k \times A_j)/\sum_j A_j$). By adopting the hierarchical approach of the PURE (Pesticide Use Risk Evaluation) decision-support system[22], we determined the risk point (RP^k) in an environmental compartment *k* as the log-transformed sum of all RQs in that compartment (i.e., $\mathrm{RP}^k = \log\sum_i \mathrm{RQ}_i^k$).

The overall risk score (RS) in a grid cell was then calculated as the maximum of the RPs across the four environmental compartments (i.e., $\mathrm{RS} = \max\{\mathrm{RP}^k\}$). We classified RS into four risk classes, i.e., negligible ($\mathrm{RS} \leq 0$), low ($0 < \mathrm{RS} \leq 1$), medium ($1 < \mathrm{RS} \leq 3$), and high ($\mathrm{RS} > 3$) based on the average species sensitivity distribution curve for pesticides (Supplementary Information Fig. S1) determined using the parameters reported in ref[43]. Specifically, $\mathrm{RS} \leq 0$ corresponds to less than 5% probability for any of the species to experience an effect, while $\mathrm{RS} > 3$ signifies that the probability for a random species to be affected by the pesticides is equal to 90%.

Model input data. The model input variables were determined from spatially explicit global data sets (Supplementary Information Table S1). We sourced the soil bulk density, porosity, and organic carbon content from the SoilGrids[44], which consists of globally-gridded soil profiles to 2 m depth. We estimated the soil water content at field capacity using the soil porosity, the globally-gridded soil field capacity obtained from the IGBP-DIS data set[45], air-entry suction and pore-volume distribution index λ obtained from ref[46], following the Brooks and Corey model[47] (i.e., soil water content = [field capacity / air entry suction]$^{-\lambda}$ × porosity). The soil properties used in this work were the averages along the top 2 m soil depth.

We acquired the equilibrium groundwater table depth from ref[48] and we estimated the groundwater thickness by subtracting the groundwater table depth from the soil thickness (distance to bedrock), which was sourced from the Distributed Active Archive Centre for Biogeochemical Dynamics of the Oak Ridge National Laboratory (ORNL/DAAC)[49]. The net groundwater recharge was estimated as the balance between annual rainfall and evapotranspiration. We sourced globally-gridded daily rainfall data from the CPC Global Unified Precipitation data provided by the NOAA/OAR/ESRL PSD, Boulder, Colorado, USA[50] and the monthly actual evapotranspiration from ref[51], while the atmospheric temperature was sourced from the Global Historical Climatology Network - Daily (GHCN-Daily) data set[52]. We obtained the globally-gridded terrain slope maps from the Harmonized World Soil Database v1.2[53].

The AI physicochemical and ecotoxicological properties were obtained from the PPDB[41] database and other previous literature[54-59] (see Supplementary Information Table S2 for details).

Output maps and data analyses. We ultimately produced three output maps[60] gridded at 5 arc-minutes resolution (approximately 10 km at the equator): the first is the RS map showing the exposure of agricultural land to pesticide pollution (Fig. 1); the second is the AI count map quantifying the number of AIs posing pollution risk to agricultural land and showing the exposure of the environment to pesticide mixtures (Fig. 2); and the third is the regions of concern map identifying locations susceptible to pesticide pollution upon meeting the selected criteria described below (Fig. 3). To produce these maps, we selected 1,199,195 grid cells with agricultural land using the harvested area maps of the 10 crop classes distributed along with PEST-CHEMGRIDS[20], which were originally produced by ref[21] and ref[61]. Among the selected grid cells, 2,408 cells (≈0.2%) were neglected due to insufficient input data for computing the RS values and hence, we modelled in total 38.54 million km^2 of agricultural land. For the AI count map, we considered an AI to pose a pollution risk if any of its RQ_i^k values were greater than 1, while the regions of concern were identified against water scarcity and biodiversity indicators.

We used the physical quantity risk indicator reported in AQUEDUCT-v2.1[14] to locate areas suffering from high water risk. The physical quantity risks measure the risks related to the availability and variability of water supply; higher values indicate higher water risks. A grid cell is considered at high water risk when its physical quantity risk exceeded 4. To identify areas bearing high biodiversity, we used the geographically-gridded species richness maps for tetrapods, which include mammals[16], birds[15], reptiles[18], and amphibians[17]. We considered a grid cell to have high biodiversity when the total number of species in that grid cell is greater than the 75th percentile of global values (i.e., 323 species). We classified countries into different income groups according to the definition in FAOSTAT[2] (Supplementary Information Table S3).

Finally, we integrated the pesticide pollution risk, water scarcity and biodiversity indicators to identify regions of concern. We assigned 'no concern' to all grid cells with RS ≤ 0 and 'concern level (4 – N)' to grid cells with RS > 0 and satisfied N criteria, which are (1) high pesticide pollution risk, i.e., RS > 3; (2) high water risk, i.e., the physical quantity risk > 4; and (3) high biodiversity, i.e., the total number of species > 75^{th} percentile of global values.

Uncertainty and data quality. We quantified the reliability of our estimates by performing a global sensitivity analysis for 11 selected input variables that include AI application rates, soil properties (bulk density, porosity, water content, and organic carbon content), groundwater characteristics (water table depth, groundwater thickness, and net recharge rate), slope angle, and hydroclimatic variables (rainfall and atmospheric temperature). We assumed all variables can span between ±50% of the reference values obtained from global data sets. For AI application rates, we tested ranges that span between +50% of the high estimates and -50% of the low estimates provided in PEST-CHEMGRIDS. We sampled randomly across the variables space using a uniform distribution and we conducted a total of 50,000 model realisations per grid cell (i.e., in total 5.98×10^{10} realisations).

Within the tested variable space, we determined the certainty index (*CI*) [60] of a grid cell as the probability for that grid cell to fall into the risk class estimated in the RS map in Fig. 1. Hence, $CI = 0$ indicates low certainty and $CI = 1$ indicates high certainty. We find that the estimated risks (Fig. 1) in approximately 22% of grid cells are highly certain (i.e., $CI = 1$, Supplementary Information Fig. S3a, with only less than 9% of grid cells having low certainty (i.e., $CI < 0.6$).

For grid cells with $CI < 1$, we determined the variable that has the highest contribution to the uncertainty by using AMAE and AMAV indices[62], which measure the relative contribution of variables to the mean and variance of the model output, respectively. Among all tested variables, AI application rates have the greatest control over uncertainties in more than 42% of grid cells (Supplementary Information Fig. S4). Hence, to compute the quality of our estimates (*QI*) [60], we combined *CI* with the data quality of PEST-CHEMGRIDS (QI_{APR}), i.e., $QI = (CI + QI_{APR})/2$. PEST-CHEMGRIDS provides AI- and crop- specific quality indices, and hence we compute the overall QI_{APR} as the average quality weighted by the application rates. In this work, our estimates have mid to high quality in 93% of grid cells (i.e., $QI \geq 0.6$, Supplementary Information Fig. S3b.

Assumptions and limitations. The pesticide pollution risk presented in this study may be overestimated because: (1) it assumes a single application at an annual rate, (2) it assumes all fields are adjacent to surface water bodies, (3) it assumes maximum exposure of non-target organisms in time and in space, and (4) it assumes no loss due to drift and interception by crops. In this study, pesticides were assumed to reach the soil as a result of direct deposition, rainfall washing of crop leaves, and crop debris fall regardless of the application methods. We presume that common practices such as spraying may lead to pesticide drift and potentially diluting its concentration and delaying the time pesticides eventually reach soil after spraying. We also identified limitations that can lead to underestimating the risks. First, our assessment did not consider legacy pollution from AIs that were banned prior to 2015. For example, atrazine was not included in the calculation of risk scores in the European Union countries that have banned its use before 2015. However, many field studies have reported the high detection frequency of atrazine and its degradation products in European soils despite its ban about a decade ago[63]. Second, we did not account for the pollution risks of pesticide degradation products, which may still be toxic and be more persistent than the parent molecules[64]. Third, the calculated PECs were non-cumulative and not dynamic in time, i.e., we did not consider the effect of accumulation of pesticides and their degradation products over time, and thus may not fully capture the pervasiveness of certain AIs. Fourth, we did not account for the synergistic effects of pesticide mixtures[65] as there is very limited data on the ecotoxicity of pesticide mixtures and only a small number of organisms have been tested for PNECs.

References

36 Baker, N. T. *Estimated Annual Agricultural Pesticide Use by Major Crop or Crop Group for States of the Conterminous United States, 1992–2016* https://dx.doi.org/doi:10.5066/F7NP22KM (U.S. Geological Survey, Reston, VA, 2018).

37 Gutsche, V. & Rossberg, D. SYNOPS 1.1: a model to assess and to compare the environmental risk potential of active ingredients in plant protection products. *Agric. Ecosyst. Environ.* **64**, 181-188 (1997).

38 Röpke, B., Bach, M. & Frede, H. DRIPS-a decision support system estimating the quantity of diffuse pesticide pollution in German river basins. *Water Sci. Technol.* **49**, 149-156 (2004).

39 Waitz, M., Freijer, J., Kreule, P. & Swartjes, F. *The VOLASOIL risk assessment model based on CSOIL for soils contaminated with volatile compounds*. Report No. RVIM Report No. 715810014, 189 (National Institute of Public Health and The Environment, Bilthoven, The Netherlands, 1996).

40 European Chemicals Bureau. Technical Guidance Document on Risk Assessment in support of Commission Directive 93/67/EEC on Risk Assessment for new notified substances, Commission Regulation (EC) No 1488/94 on Risk Assessment for existing substances, and Directive 98/8/EC of

the European Parliament and of the Council concerning the placing of biocidal products on the market (Institute for Health and Consumer Protection, Italy, 2003).

41 Lewis, K. A., Tzilivakis, J., Warner, D. J. & Green, A. An international database for pesticide risk assessments and management. *Hum. Ecol. Risk. Assess.: An Int. J.* **22**, 1050-1064 (2016).

42 European Commission. Directive 2006/118/EC of the European Parliament and of the Council of 12 December 2006 on the protection of groundwater against pollution and deterioration. *Official Journal of the European Union* **L 372**, 19-31 (2006).

43 Nagai, T. Ecological effect assessment by species sensitivity distribution for 68 pesticides used in Japanese paddy fields. *J. Pestic. Sci.* **41**, 6-14 (2016).

44 Hengl, T. *et al.* SoilGrids250m: Global gridded soil information based on machine learning. *PLoS One* **12**, 1-40 (2017).

45 Global Soil Data Task. Global Soil Data Products CD-ROM Contents (IGBP-DIS) Data Set. Oak Ridge National Laboratory Distributed Active Archive Center, Oak Ridge, Tennessee, U.S.A. http://dx.doi.org/10.3334/ORNLDAAC/565 (2014).

46 Dai, Y. *et al.* A global high-resolution dataset of soil hydraulic and thermal properties for land surface modeling. *J. Adv. Model. Earth Syst.* **11**, 2996-3023 (2019).

47 Brooks, R. H. & Corey, A. T. Properties of porous media affecting fluid flow. *J. Irrig. Drain. Div.* **92**, 61-90 (1966).

48 Fan, Y., Li, H. & Miguez-Macho, G. Global patterns of groundwater table depth. *Science* **339**, 940-943 (2013).

49 Pelletier, J. *et al.* Global 1-km Gridded Thickness of Soil, Regolith, and Sedimentary Deposit Layers. Oak Ridge National Laboratory Distributed Active Archive Center, Oak Ridge, Tennessee, U.S.A. https://doi.org/10.3334/ORNLDAAC/1304 (2016).

50 NOAA/OAR/ESRL PSD. CPC Global Unified Precipitation dataset. Physical Sciences Laboratory, Boulder, Colorado, USA https://psl.noaa.gov/data/gridded/data.cpc.globalprecip.html (2019).

51 Zhang, Y. *et al.* Monthly global observation-driven Penman-Monteith-Leuning (PML) evapotranspiration and components v2. CSIRO Data Collection https://doi.org/10.4225/08/5719A5C48DB85 (2016).

52 Menne, M. J., Durre, I., Vose, R. S., Gleason, B. E. & Houston, T. G. An overview of the global historical climatology network-daily database. *J. Atmos. Ocean. Technol.* **29**, 897-910 (2012).

53 Fischer, G. *et al.* Harmonized World Soil Database v1.2. Global agro-ecological zones assessment for agriculture (GAEZ 2008) IIASA, Laxenburg, Austria and FAO, Rome, Italy http://www.fao.org/soils-portal/data-hub/soil-maps-and-databases/harmonized-world-soil-database-v12/en/ (2008).

54 US-EPA. *Pesticide Fact Sheet, Aminopyralid.* Report No. 7501C (United States Office of Prevention, Pesticides Environmental Protection and Toxic Substances Agency, U.S.A., 2005).

55 Herner, A. E. The USDA-ARS pesticide properties database: a consensus data set for modelers. *Weed Technol.* **6**, 749-752 (1992).

56 Mao, L., Zhang, L., Zhang, Y. & Jiang, H. Ecotoxicity of 1, 3-dichloropropene, metam sodium, and dazomet on the earthworm Eisenia fetida with modified artificial soil test and natural soil test. *Environ. Sci. Pollut. Res.* **24**, 18692-18698 (2017).

57 National Institutes of Health, Health & Human Services. ChemIDplus. U.S . National Library of Medicine https://chem.nlm.nih.gov/chemidplus/ (2019).

58 Australian Pesticides and Veterinary Medicine Authority. *Public release summary on the Evaluation of the New Active Saflufenacil in the Product SHARPEN WG HERBICIDE (Previously Heat Herbicide)*. Report No. APVMA Product Number 62853 (APVMA, Australia, 2012).

59 US-EPA. *Pesticide Fact Sheet, Saflufenacil*. Report No. 7505P (United States Office of Prevention, Pesticides Environmental Protection and Toxic Substances Agency, U.S.A., 2009).

60 Tang, F. H. M., Lenzen, M., McBratney, A. & Maggi, F. Global pesticide pollution risk data sets. figshare http://dx.doi.org/10.6084/m9.figshare.10302218 (2021).

61 Ramankutty, N., Evan, A. T., Monfreda, C. & Foley, J. A. Farming the planet: 1. Geographic distribution of global agricultural lands in the year 2000. *Global Biogeochem. Cycles* **22**, 1 (2008).

62 Dell'Oca, A., Riva, M. & Guadagnini, A. Moment-based metrics for global sensitivity analysis of hydrological systems. *Hydrol. Earth Syst. Sci.* **21**, 6219–6234 (2017).

63 Hvězdová, M. *et al.* Currently and recently used pesticides in Central European arable soils. *Sci. Total Environ.* **613**, 361-370 (2018).

64 Fenner, K., Canonica, S., Wackett, L. P. & Elsner, M. Evaluating pesticide degradation in the environment: blind spots and emerging opportunities. *Science* **341**, 752-758 (2013).

65 Deneer, J. W. Toxicity of mixtures of pesticides in aquatic systems. *Pest Manag. Sci.* **56**, 516-520 (2000).

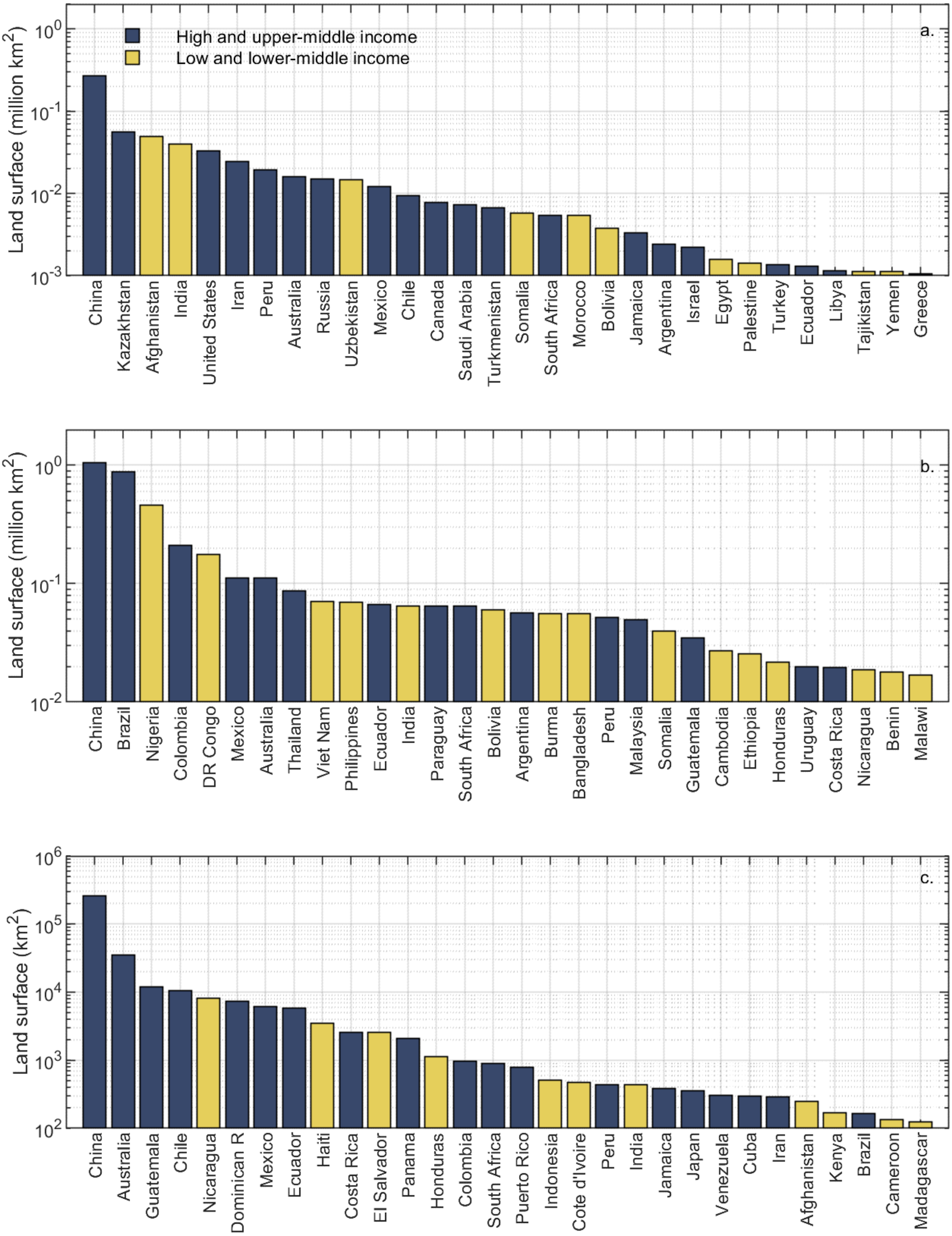

Extended Data Fig. 1 The top 30 countries susceptible to high pesticide pollution risk. a., The land area subject to low quantity and high variability of water supply and high risk of pollution by pesticide mixtures (i.e., RS > 3 and AI count > 1). **b.,** The land area bearing high biodiversity and subject to high risk of pollution by pesticide mixtures (i.e., RS > 3 and AI count > 1). **c.,** The land area inhabited by at least one endangered and critically endangered amphibian species and subject to pollution risk by pesticide mixtures (RS > 0 and AI count > 1).

546

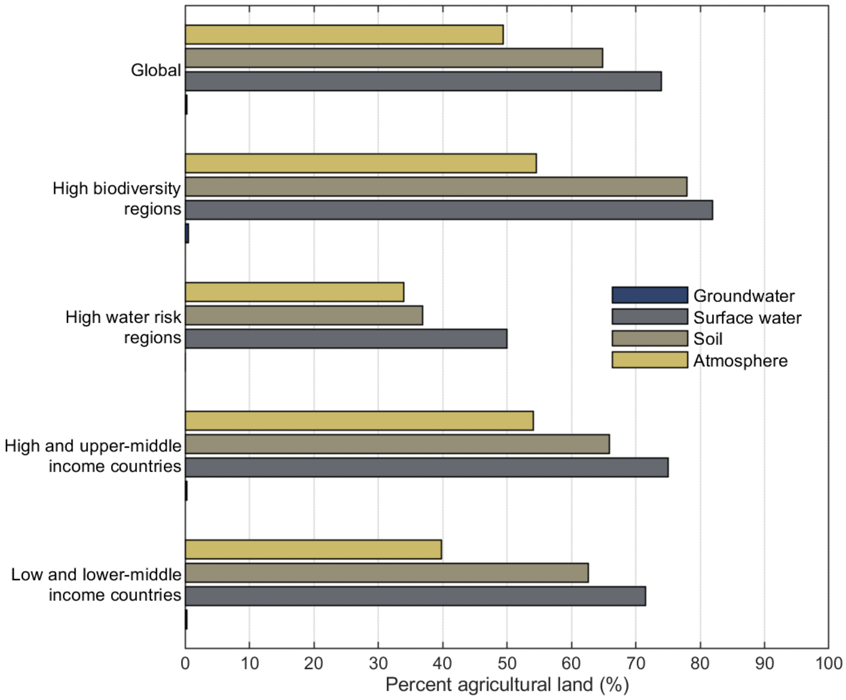

Extended Data Fig. 2 The extent of pesticide pollution risk in groundwater, surface water, soil, and atmosphere expressed as percent agricultural land. For example, surface water within 74% of global agricultural land is at some risk of pesticide pollution. High water risk regions refer to places suffering from low quantity and high variability of water supply defined as in AQUEDUCT-v2.1 database.